# Ultraviolet picosecond optical pulse generation from a mode-locked InGaN laser diode

S. Gee[a] and J. E. Bowers
*Electrical and Computer Engineering Department, University of California, Santa Barbara, Santa Barbara, California 93106*

(Received 7 May 2001; accepted for publication 20 July 2001)

Ultraviolet optical pulses were generated by actively mode locking an external cavity InGaN laser at a wavelength of 409 nm with a temporal pulse duration of 30 ps. The average power was 2 mW and the time–bandwidth product was 1.2. Dynamic detuning plays a major role in pulse development. © *2001 American Institute of Physics.* [DOI: 10.1063/1.1405432]

Mode-locked semiconductor lasers are an important source for generating subpicosecond optical pulses.[1] Recent developments of GaN-based semiconductor lasers have made it possible for semiconductor lasers to cover the entire wavelength range from ultraviolet to infrared.[2] Ultrashort optical pulses of wavelength near 400 nm are typically generated by the frequency doubling of mode-locked Ti:sapphire lasers or dye laser output. In view of this fact, mode-locked semiconductor lasers at these wavelengths are very attractive light sources due to their compact and efficient nature. In addition, subsequent frequency doubling of these semiconductor lasers output can generate light at ~200 nm for potential application of laser marking and lithography.[3] In this letter, we report on mode-locked InGaN lasers.

The experimental setup is shown in Fig. 1. The cavity is composed of a diffraction grating of groove density 1200 g/mm and a semiconductor optical amplifier (SOA). The SOA was obtained by $SiO_2Ta_2O_5$ double-layer antireflection (AR) coating a cleaved facet of a commercial ridge waveguide multiple-quantum-well InGaN diode from Nichia Corp. (model: NLHV500A). The reflectivity was estimated to be less than $10^{-3}$ using the Hakki–Paoli method.[4] In order to suppress the Fabry–Pérot mode caused by imperfect AR coating on the SOA facet, the diffraction grating was employed to limit the spectral width. The laser output was obtained from a 50% beam splitter instead of using the zero-order diffraction of the grating owing to its low efficiency. The active mode locking was realized by driving the SOA with 20 mW of rf power at the cavity round-trip frequency combined with 43 mA of dc current using a bias tee. The repetition rate was 720 MHz and the average output power was 2 mW.

Figure 2(a) shows the optical intensity spectrum of the mode-locked laser output showing a spectral width of 0.023 nm at the center wavelength of 408.5 nm. Due to the imperfect AR coating on the SOA, Fabry–Pérot mode still exists with 0.035 nm of modulation period. Figure 2(b) shows the temporal intensity profile of the output pulse measured by a syncroscan streak camera with resolution of 10 ps. The pulse has a steep rise and slow decay with the temporal width of 30 ps, indicating a time–bandwidth product (TBP) of 1.2. This nontransform-limited time–bandwidth product is due to the nonlinear chirp imposed upon the optical pulses owing to gain dynamics of the SOA and the multiple pulse formation due to the imperfect antireflection coating on the SOA facet.[5,6]

The asymmetric temporal pulse shape and the subsequent satellite pulse formation can be explained by the dynamic detuning effect in active mode locking.[7] In active mode locking, the peak of the optical pulse occurs not at the peak in the gain wave form but a little bit earlier than the gain peak in the absence of the optical pulse. As a short optical pulse is amplified in the SOA, the pulse becomes more and more intense and eventually starts to saturate the gain. The front part of the pulse sees more gain and is amplified more than the back part of the pulse. Therefore, the pulse shape becomes asymmetric. This effect also moves the pulse earlier in the gain modulation period. The dynamic detuning continues until the change in gain due to gain saturation is balanced by a change in gain due to the applied gain wave form. As the pulse moves forward, the slope of the gain seen by the pulse becomes steeper owing to the sinusoidal nature of the bias current, until at some position, it balances exactly the change in gain due to gain saturation. If the pulse goes further forward, the back part of the pulse starts to see more gain due to the sinusoidal modulation and the pulse develops an elongated tail or even a satellite pulse. To support this explanation, the cavity length dependence of mode locking was investigated. Figure 3 is the series of streak camera images for different cavity length settings while the rf bias current frequency is held constant at 720 MHz. The shadowed curve is the bias current wave form, which was determined by measuring the spontaneous emission of the SOA. The amount of cavity length change is translated into

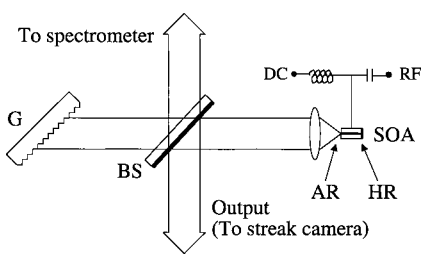


FIG. 1. Laser setup. SOA: semiconductor optical amplifier; BS: beam splitter; G: diffraction grating; AR: anti reflection coating; and HR: high-reflection coating.

[a]Electronic mail: gee@opto.ucsb.edu

 

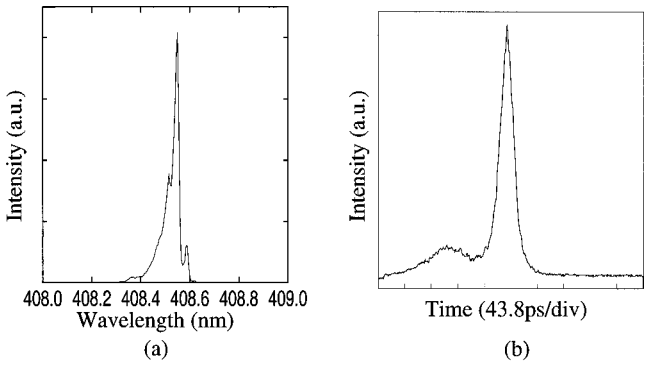


FIG. 2. Typical mode-locked output: (a) optical intensity spectrum (spectral width 0.023 nm) and (b) streak camera images (earlier times to the right, pulse width 30 ps, TBP 1.2).

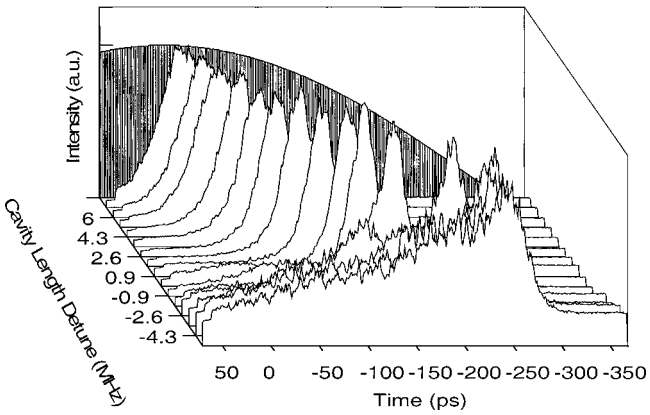


FIG. 3. Cavity length detuning characteristics: Streak images vs detuning.

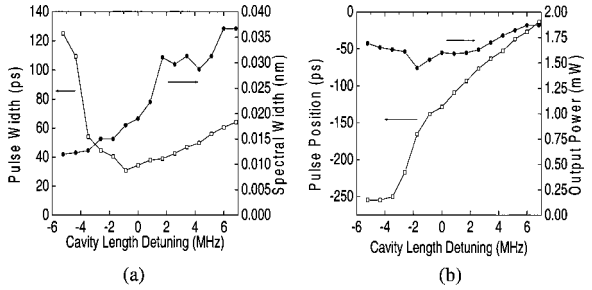


FIG. 4. Cavity length detuning characteristics: (a) pulse width and spectral width vs detuning and (b) pulse position and output power vs detuning.

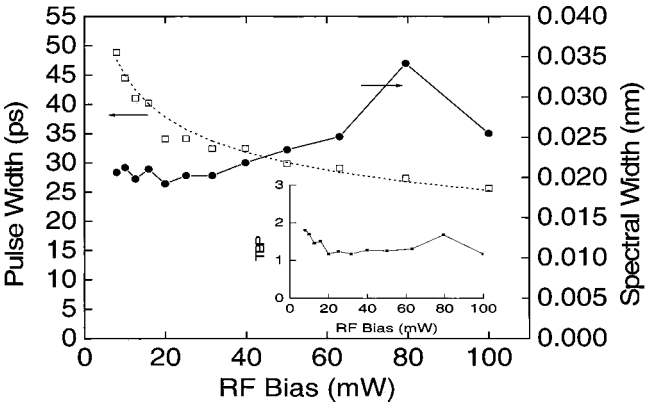


FIG. 5. Rf bias characteristics: pulse width and spectral width vs rf bias. The inset is TBP vs rf bias.

the negative of the cavity round-trip frequency change so that it mimics the rf bias frequency change for the fixed cavity length. It is easily seen that the optical pulse is always ahead of the peak of the gain. As the cavity length is reduced, the pulse moves forward relative to the gain. It should be noted that the motive force of repositioning the pulse is not in the cavity length detuning but the dynamic detuning effect. It can be easily understood if we consider the fact that the amount of the cavity length change in each plot is 250 $\mu$m, corresponding to 1.7 ps of delay while the actual pulse position change is more than 20 ps. The shortest pulse occurs at an early enough position of the gain so as to balance the higher level of saturation with the slope of the applied gain. As the pulse goes further forward, the back part of the pulse starts to see more gain and the pulse develops an elongated tail. When the cavity length is increased, the pulse moves backward and the pulse width becomes gradually longer [Fig. 4(a)]. The pulse-width broadening is faster for cavity length decreasing than increasing as predicted by earlier theory.[7] It should also be noted that as the pulse moves backward it sees more net gain due to the applied gain modulation and it resulted in a gradual increase of output power [Fig. 4(b)].

Figure 5 shows the rf bias current dependence of the pulse width. The pulse width decreases as the rf bias increases, showing that the pulse width is inversely proportional to the fourth root of the modulation strength while the time–bandwidth product almost remains constant (the dotted line is the fit for the negative fourth root of the rf bias).[8]

In summary, we have demonstrated the generation of ultraviolet picosecond optical pulses at 409 nm with a temporal duration of 30 ps from an actively mode-locked external cavity InGaN laser system. It was found that the dynamic detuning effect of active mode locking plays a major role in pulse development in the laser cavity and the laser behavior matches well with the classical active mode-locking model developed by Kuizenga and Siegman.[8] It is expected that an improved AR coating on the SOA facet will help to produce shorter pulse generation and subsequent amplification will boost the output power to expand the range of applications.

[1] P. J. Delfyett, L. T. Florez, N. Stoffel, T. Gmitter, N. C. Andreadakis, Y. Silberberg, J. P. Heritage, and G. A. Alphones, IEEE J. Quantum Electron. **28**, 2203 (1992).
[2] S. Nakamura and G. Fasol, *The Blue Laser Diode* (Springer, Berlin, 1998).
[3] H. Endert, R. Patzel, and D. Basting, Opt. Quantum Electron. **27**, 1319 (1995).
[4] S. A. Merritt, C. Dauga, S. Fox, I.-F. Wu, and M. Dagenais, J. Lightwave Technol. **13**, 430 (1995).
[5] M. Schell, A. G. Weber, E. Scholl, and D. Bimberg, IEEE J. Quantum Electron. **27**, 1661 (1991).
[6] S. Gee, R. Coffie, G. Alphonse, J. Connolly, and P. J. Delfyett, Appl. Phys. Lett. **71**, 2569 (1997).
[7] P. A. Morton, R. J. Helkey, and J. E. Bowers, IEEE J. Quantum Electron. **25**, 2621 (1989).
[8] D. J. Kuizenga and A. E. Siegman, IEEE J. Quantum Electron. **6**, 694 (1970).